www.sciencemag.org/content/341/6153/1502/suppl/DC1

Supplementary Materials for

Cation Intercalation and High Volumetric Capacitance of Two-Dimensional Titanium Carbide

Maria R. Lukatskaya, Olha Mashtalir, Chang E. Ren, Yohan Dall'Agnese, Patrick Rozier, Pierre Louis Taberna, Michael Naguib, Patrice Simon, Michel W. Barsoum, Yury Gogotsi*

*Corresponding author. E-mail: gogotsi@drexel.edu

Published 27 September 2013, *Science* **341**, 1502 (2013)
DOI: 10.1126/science.1241488

This PDF file includes:

Materials and Methods

Synthesis of multilayer exfoliated $Ti_3C_2T_x$ MXene

$Ti_3C_2T_x$ (where T stands for surface termination, such as OH, O or F bonded to Ti atoms) was synthesized by exfoliating the corresponding MAX phases with "A" element etched away. Ti_3AlC_2 powder with particle size less than 38 μm was treated with 50% aqueous HF solution (Fisher Scientific, Fair Lawn, NJ) at room temperature (RT), for 18 h. The resulting suspensions were washed six to seven times using deionized water and separated from remaining HF by centrifuging until the pH of the liquid reached around 5. The wet sediment was moved to a wide-mouth jar by ethanol and dried in air for 3 to 4 days. Then the obtained $Ti_3C_2T_x$ was placed into capped glass vials and stored at ambient conditions for further experiments.

Electrode film preparation from the multilayer $Ti_3C_2T_x$ powder

Electrodes were prepared by mechanical processing of the pre-mixed slurry, containing ethanol (190 proof, Decon Laboratories, Inc.), $Ti_3C_2T_x$ powder, polytetrafluoroethylene (PTFE) binder (60 wt.% in H_2O, Aldrich) and onion-like carbon (OLC) *(28)*, which was added to create a conductive network in-between the particles (MXene is anisotropic: good in-sheet conductivity, poor conductivity between the sheets). Resulting electrodes which were used for all experiments contained: 85 wt. % of the $Ti_3C_2T_x$, 10 wt.% of OLC, 5 wt. % of PTFE and had thickness of 75-100 μm and mass density per unit area of 7-9 mg/cm^2.

Intercalation of multilayer exfoliated $Ti_3C_2T_x$

To intercalate $Ti_3C_2T_x$, 0.15 g of the powder was suspended in 5 ml of 30 wt.% aqueous solution of potassium hydroxide, potassium acetate, lithium acetate, sodium acetate, sodium formate, sodium citrate, and zinc sulfate; 25, 20 and 10 wt.% aqueous solution of magnesium sulfate, sodium sulfate and potassium sulfate, respectively; 30 % aqueous solutions of acetic acid, sulfuric acid, and ammonium hydroxide. Then, the mixtures were stirred for 24 h with a magnetic stirrer at room temperature, RT. Afterwards, the resulting colloidal solutions were filtered through a polyester membrane (25 mm diameter, 3 μm pore size, Osmonics Inc., Minnetonka, MN, USA) and dried in a desiccator under vacuum (< 10 Torr) at RT.

Synthesis of the few-layer $Ti_3C_2T_x$ and paper electrode preparation

To obtain few-layer $Ti_3C_2T_x$, multilayered $Ti_3C_2T_x$ was stirred with dimethyl sulfoxide (DMSO) for 18h at room temperature, then the colloidal suspension was centrifuged to separate the intercalated powder from the liquid DMSO. After decantation of the supernatant, deionized water was added to the residue in a weight ratio of MXene to water of 1:500. Then the suspension was sonicated under Ar for 4 h, and centrifuged for 1 h with 3500 rpm. At last, the supernatant was decantated and filtered using a porous MF-millipore mixed cellulose ester membrane filter (47 mm diameter, 0.025 μm pore size, Fisher Scientific, Fair Lawn, NJ, USA) and dried in a desiccator under vacuum (<10 Torr) at RT for 24 h, resulting in MXene paper that detaches easily from the membrane

and can be further used as a *free-standing electrode*. Thickness of the MXene paper varied from 2 to 20 μm. Mass density per unit area of tested electrodes was 2-3 mg/cm^2.

Chemicals used in experiments

The following ionic compounds were used for intercalation into $Ti_3C_2T_x$: potassium hydroxide (≥85.0%, Fisher Chemical, Fair Lawn, NJ, USA), potassium sulfate (certified ACS crystalline, Fisher Scientific, Fair Lawn, NJ, USA), potassium acetate (ACS reagent grade, MP Biomedicals, LLC, Solon, OH, USA), lithium acetate anhydrous (≥99%, Acros Organics, Fair Lawn, NJ, USA), sodium acetate anhydrous (≥99.0%, Alfa Aesar, Ward Hill, MA, USA), sodium formate (>99.0%, Alfa Aesar, Ward Hill, MA, USA), sodium citrate tribasic dehydrate (>98%, Sigma Aldrich, St. Louis, MO, USA), sodium sulfate anhydrous (99.7%, Acros Organics, Fair Lawn, NJ, USA), magnesium sulfate (≥99.5%, Alfa Aesar, Ward Hill, MA, USA), zinc sulfate heptahydrate (≥99.0%, Sigma Aldrich, St. Louis, MO, USA). Ammonium hydroxide (28-30 wt.% in water, Fisher Scientific, Fair Lawn, NJ, USA), acetic acid (99.8%, Acros Organics, Fair Lawn, NJ, USA), and sulfuric acid (50%, Ricca Chemical Company, Arlington, TX, USA) were also used as intercalants.

The following salts were used as electrolytes in electrochemical experiments: potassium hydroxide (≥85.0%, Fisher Chemical, Fair Lawn, NJ, USA), potassium sulfate (certified ACS crystalline, Fisher Scientific, Fair Lawn, NJ, USA), sodium acetate anhydrous (≥99.0%, Alfa Aesar, Ward Hill, MA, USA), sodium hydroxide (≥98%, Alfa Aesar, Shore Road, Heysham, Lancs UK), sodium nitrate (≥99%, Sigma Aldrich, St. Louis, MO, USA), magnesium nitrate hexahydrate (≥99%, Sigma Aldrich, St. Louis, MO, USA), magnesium sulfate (≥99.5%, Alfa Aesar, Ward Hill, MA, USA), aluminum sulfate hydrate (≥98.0%, Fluka, St. Louis, MO, USA), ammonium sulfate (≥99.0%, Sigma Aldrich, St. Louis, MO, USA), and lithium sulfate (≥98.5%, Sigma Aldrich, St. Louis, MO, USA).

Activated carbon (AC) counter electrodes

Activated carbon film electrodes were prepared following the same procedure as for the $Ti_3C_2T_x$ electrodes, but without any conductive additive. Resulting AC electrodes composition was 95 wt. % of YP-50 activated carbon (Kuraray, Japan) and 5 wt. % of the PTFE. They had thickness of 100-150 μm and mass density per unit area of 10-25 mg/cm^2.

Electrochemical set-up

All electrochemical measurements were performed in 3-electrode Swagelok cells, where MXene served as working electrode, over-capacitive activated carbon films were used as counter electrode and Ag/AgCl in 1 M KCl as a reference in order to precisely control electrochemical potentials.

Electrochemical measurements

Cyclic voltammetry, electrochemical impedance spectroscopy and galvanostatic cycling were performed using a VMP3 potentiostat (Biologic, France).

*Cyclic voltammetry w*as performed using scan rates from 1 mV/s to 1000 mV/s. Diapasons of cycling were chosen using the following principles:

1) As starting potential, open circuit potential right after assembly of the cell was chosen.
2) Minimum potential was chosen by subsequent CV series with increasing lower limit, with the end at the lower limit minimum potential, at which no electrolyte decomposition was observed.

The reason for choosing OCP as upper limit is to avoid oxidation of the material in aqueous electrolytes which would lead to higher resistance and lower resulting capacitance (Fig. S3).

Electrochemical impedance spectroscopy (EIS) was performed at open circuit potential with a 10 mV amplitude between 10 mHz and 200 kHz.

Galvanostatic cycling was performed at 0.1 and 1 A/g with potential limits selected specifically for each electrolyte: from -0.5 to 1 V vs. Ag/AgCl for 1 M KCl, from 0 to -0.7 V vs. Ag/AgCl for 1 M $MgSO_4$ and 1 M NaOAc.

Physical characterization

X-Ray diffraction patterns were recorded with a powder diffractometer (Rigaku SmartLab) using Cu K_α radiation (λ = 1.54 Å) with 0.01° 2θ steps and 6 s dwelling time. *Scanning electron microscopy* (SEM) and *energy dispersive X-ray spectroscopy* (EDX) analysis were performed on Zeiss Supra 50 VP (Carl Zeiss SMT AG, Oberkochen, Germany).

In-situ electrochemical XRD

XRD patterns of the $Ti_3C_2T_x$ electrodes were collected on a Brucker D8 diffractometer using a Cu Kα radiation (λ=1.5406 Å) in the range 2θ=5–20° with a step of 0.02°. The sample was placed in a 2-electrode Swagelok-type cell and covered with a Mylar window to avoid electrolyte evaporation, allowing in-situ XRD recording (cell from LRCS, Amiens University). A MXene film, a mixture of 90% $Ti_3C_2T_x$, 5% PTFE and 5% carbon black served as the working electrode, and was pressed on a nickel foam current collector and dried at 120 °C. Over-capacitive activated carbon films were used as counter electrode. Cyclic voltammetry advanced technique was used in order to control the cell potential. The scans were recorded each 0.2 V after linear sweep at 1 mV/s.

Supplementary Text

Electrochemical behavior of the MXene in $MgSO_4$ electrolyte

For salts like $MgSO_4$, maximum capacity was only reached after 48 h as shown in Fig. S5, where it is obvious that the CV area increases steadily with time. Moreover, when *in-situ* XRD patterns of $Ti_3C_2T_x$ powders simply soaked in a $MgSO_4$ solution (green curve in Fig. S1B) are compared to those that were obtained for a fully charged cell (Fig. 3B), it is clear that intercalation led to a large shift of the (0002) peak from its initial position (Fig. S1B). The *c* value changes for the former were the same as for chemically intercalated $Ti_3C_2T_x$ with $MgSO_4$. It is thus reasonable to assume that the intercalation of Mg^{2+} ions into $Ti_3C_2T_x$ can be additionally assisted by the application of an external potential and even then, the kinetics remain sluggish (Fig. S5). Why this is the case is not entirely clear at this time, but can be due to the acidic nature of the $Ti_3C_2T_x$ alluded to above and/or the presence of a larger-sized solvation shell around the Mg^{2+}

ions. A step on the CV at -0.4 to -0.5 V suggests a two-stage intercalation or a reversible redox process, the mechanism of which needs further study. Moreover, EDX studies (Table S2) indicate that amount of Mg content in the sample synthesized by purely chemical intercalation in $MgSO_4$ is 4 times lower as compared to Mg content in electrochemically cycled $Ti_3C_2T_x$ sample.

Theoretical specific surface area calculations for $Ti_3C_2(OH)_2$ and estimation of the number of layers in multilayer exfoliated $Ti_3C_2T_x$ and few-layer $Ti_3C_2T_x$:

Area of one lattice = Lattice parameters *a* x *b x sin (60°)*= 3.0581 Å x 3.0588 Å x $(3)^{0.5}/2$ x 10^{-20}= 8.1E-20 m^2

Each layer in the cell has 3Ti, 2C, 2O, and 2H.

Then the weight of the layer in the cell = [201.64 g/mole] / [6.023E23 atoms/mole] = 3.3478E-22 g

The SSA = 8.1E-20E-20/3.3478E-22= 241.97 m^2/g (one side)

Then the SSA of a *Single* layer (2 sides) of $Ti_3C_2(OH)_2$ will be 483.94 m^2/g.

Hint: *These calculations ignore the presence of edges and defects.*

Experimental SSA for MXene paper and its corresponding number of layers**:**

98 m^2/g using N_2 → ~ 5 layers

128 m^2/g using CO_2 → ~ 4 layers

167 m^2/g using Ar → ~ 3 layer

For stacked $Ti_3C_2T_x$, experimental SSA calculated from nitrogen sorption, is 23 m^2/g, which translated to ~ 21 layers in an average MXene lamella.

Calculations of volumetric power and energy densities of electrode and cell:

$C=(\int jdV)/s/V$ $[F/cm^3]$

$E=0.5\ C*V^2/3600$ $[Wh/cm^3]$

$P=E*s/V*3600$ $[W/cm^3]$

where *C*-normalized capacitance [F/cm^3], *j*-current density [A/cm^3], *s*-scan rate [V/s], *V*-voltage window [V], similarly calculations of the gravimetric properties was performed, but gravimetric capacitance and current density were used instead.

.

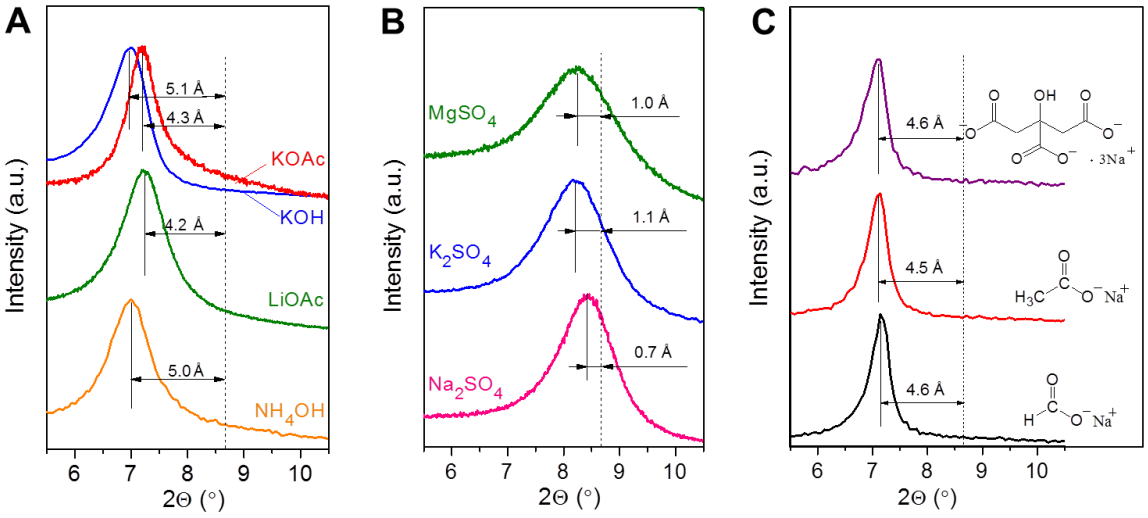

Fig. S1. X-ray diffractions patterns of various salts: (A) compounds which form basic solutions when dissolved in water, (B) sulfate salts which form nearly neutral solutions when dissolved in water and, (C) Na-salts with different organic anions. In all figures the location of the $Ti_3C_2T_x$ peak before immersion in the salt solutions is depicted by dashed vertical line. In all cases, the c-lattice parameter increases by the values shown and ranged from a high of 5 Å to a low of 0.7Å.

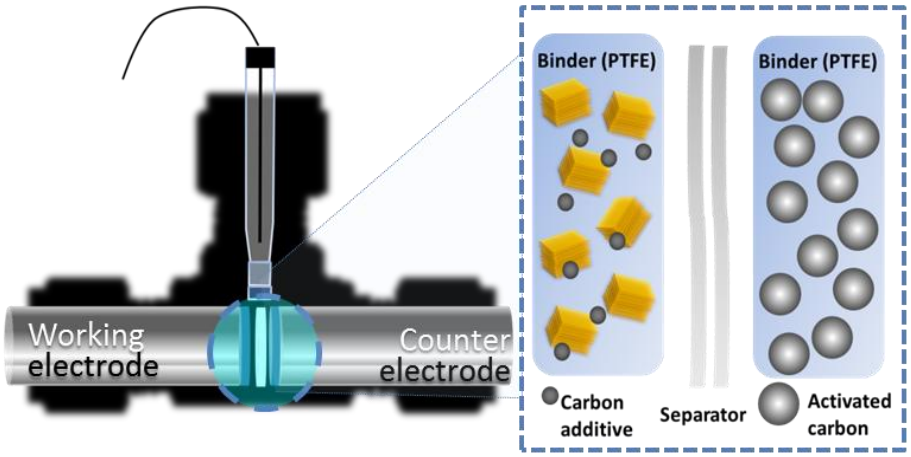

Fig. S2. Schematics of the electrochemical testing set-up: 3-electrode Swagelok cell, with multilayer $Ti_3C_2T_x$ as working electrode (yellow elements)

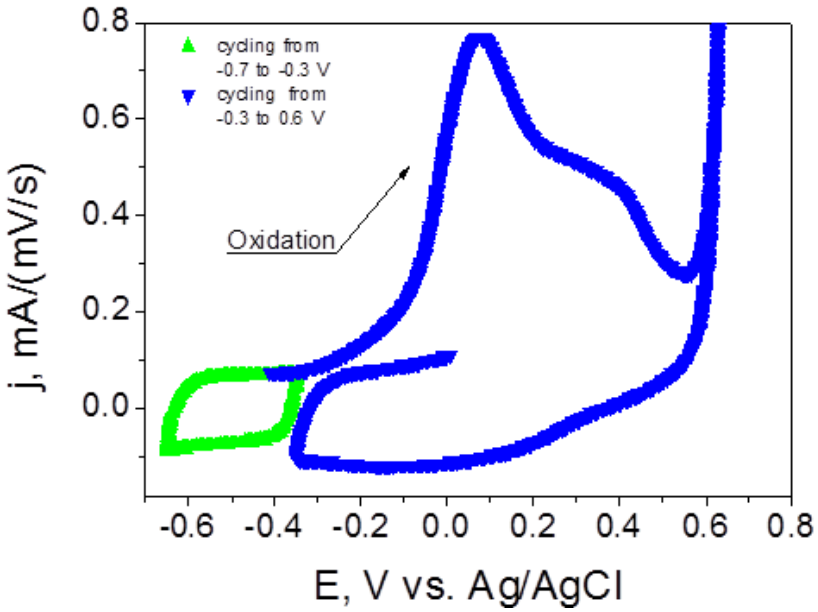

Fig. S3. Cyclic voltammetry of the $Ti_3C_2T_x$ in different potential windows (scan rate 10 mV/s) in 1 M KOH.

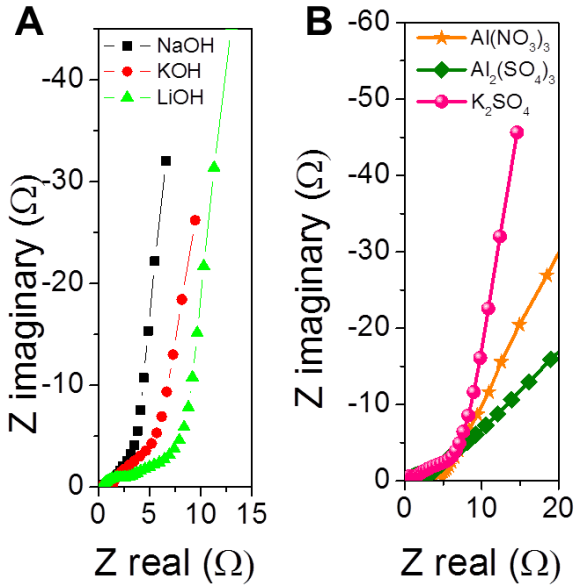

Fig. S4. Nyquist plots of the $Ti_3C_2T_x$ electrodes in (A) NaOH, KOH, LiOH and (B) K_2SO_4, $Al_2(SO_4)_3$, $Al(NO_3)_3$ solutions.

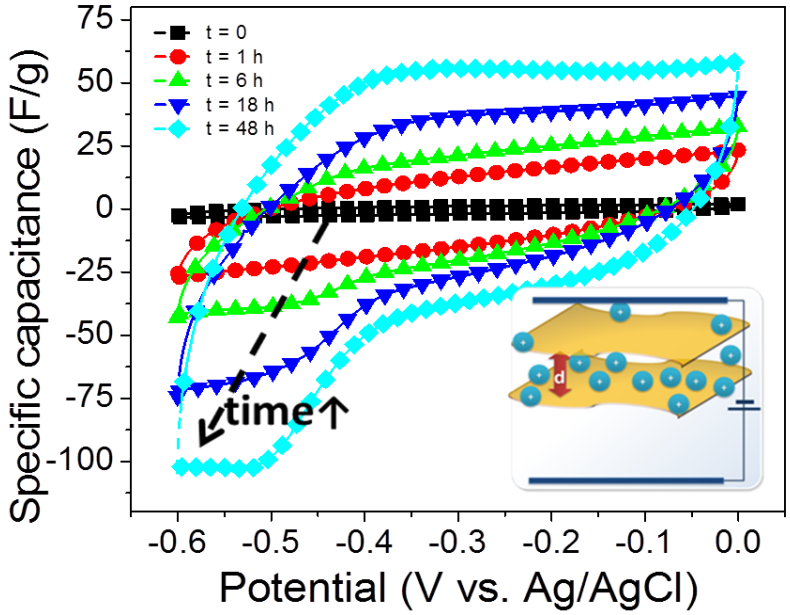

Fig. S5. CVs of $Ti_3C_2T_x$ in 1M $MgSO_4$ electrolyte collected after 0 h, 1 h, 6 h, 18 h and 48 h of cycling. Inset: schematic illustration of the electrochemically induced cation intercalation between layers of MXene.

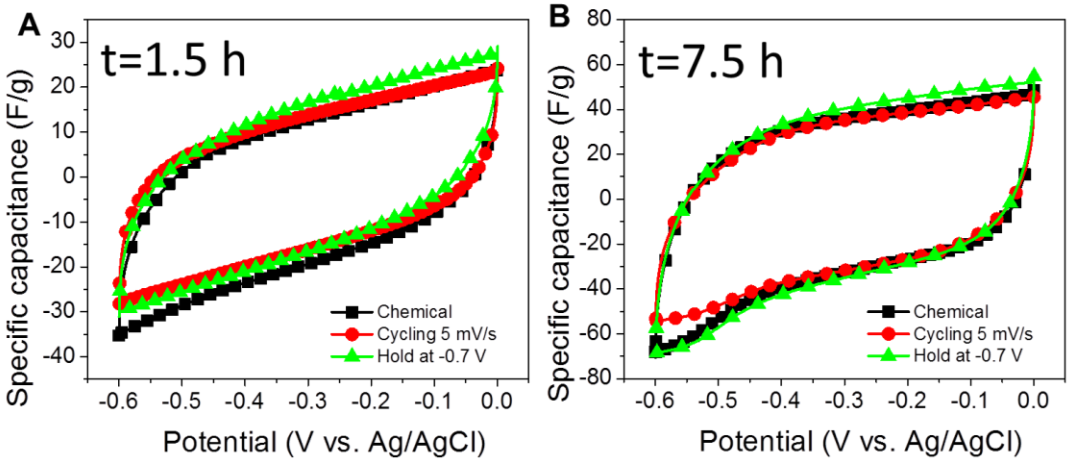

Fig. S6. CVs of $Ti_3C_2T_x$ in 1M $MgSO_4$ electrolyte collected during different cycling regimes: 1) Chemical intercalation, screening cycling in-between; 2) Continuous cycling at 5 mVs 3) Holding at -0.7 V, screening cycling in-between; collected after (A) 1.5 h, (B) 7.5 h from the beginning of the experiment.

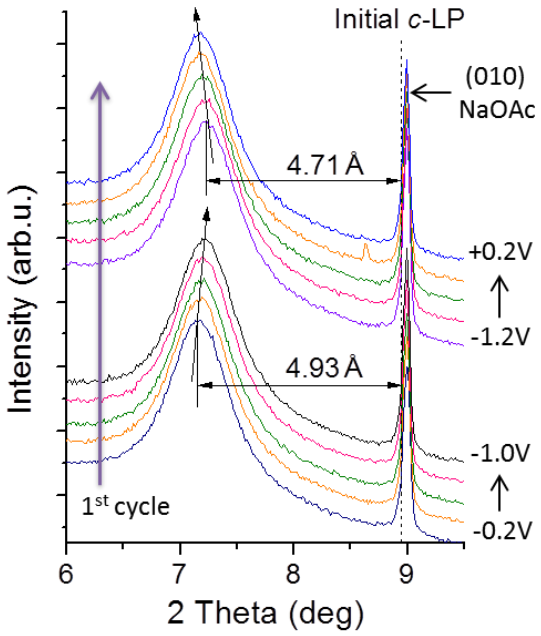

Fig. S7. Electrochemical *in-situ* X-ray diffraction study of $Ti_3C_2T_x$ in 3M solution of sodium acetate. Arrows indicate the direction of (0002) peak shift.

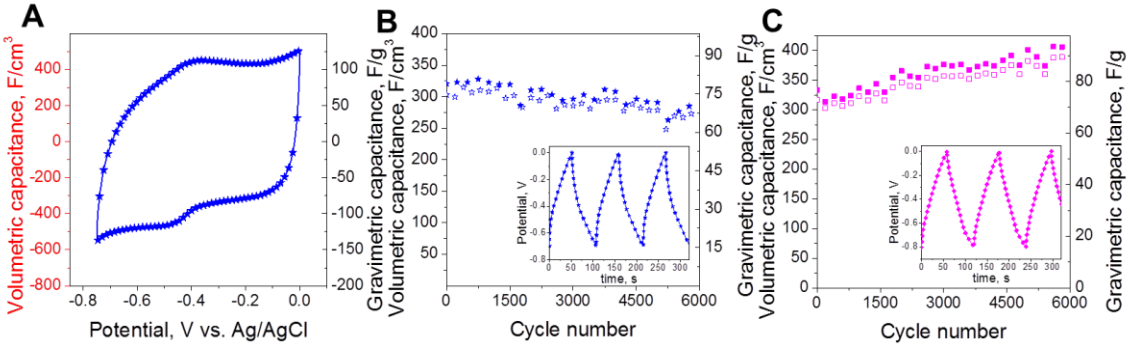

Fig. S8. Electrochemistry of $Ti_3C_2T_x$ paper. (A) Cyclic voltammograms in 1M $MgSO_4$ electrolyte; Capacitance retention test of MXene paper in 1 M $MgSO_4$ (B) and 3 M NaOAc (C) and Inset: gavlanostatic cycling data of $Ti_3C_2T_x$ paper in $MgSO_4$ (B) and NaOAc (C).

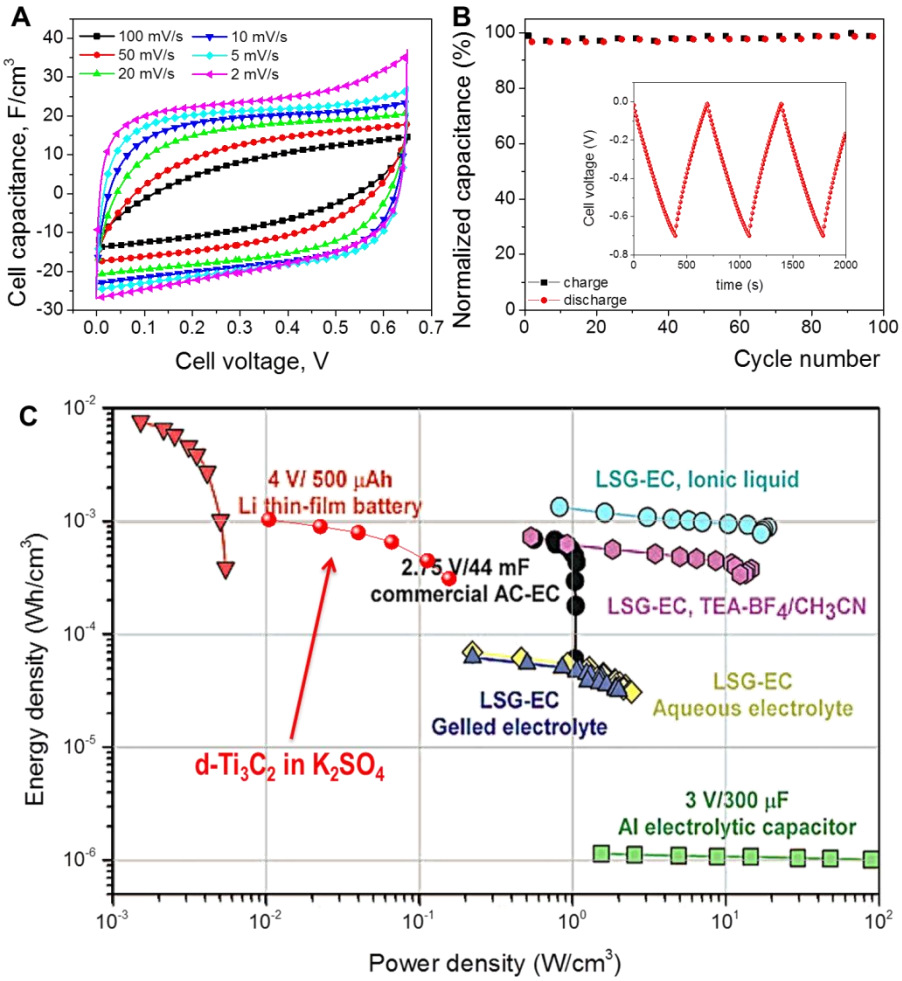

Fig. S9. $Ti_3C_2T_x$ paper cell performance in K_2SO_4: (A) Cyclic voltammetry data at different scan rates; (B) Capacitance retention test. Inset: gavlanostatic cycling data collected at 1 A/g; (C) Energy and power densities of MXene paper cell compared with commercially available aluminum electrolytic capacitors, and a lithium thin-film battery *(29)*

Table S1. Changes in *c*-lattice parameters after intercalation of $Ti_3C_2T_x$ with ions. Value of Δ (third column) indicates the increase of the *c*-lattice parameter of $Ti_3C_2T_x$ after intercalation (second column) compared to initial *c* value of 20.3 Å.

Intercalant	***c*, Å**	**Δ, Å**
Intercalants which possess a basic character when dissolved in water		
Potassium hydroxide	25.4	5.1
Ammonium hydroxide	25.3	5.0
Sodium carbonate	25.3	5.0
Sodium hydroxide	25.1	4.8
Sodium formate	24.9	4.6
Sodium citrate	24.9	4.6
Sodium acetate	24.8	4.5
Potassium acetate	24.6	4.3
Lithium acetate	24.5	4.2
Intercalants which possess a nearly neutral character when dissolved in water		
Zinc sulfate	21.7	1.4
Potassium sulfate	21.4	1.1
Magnesium sulfate	21.3	1.0
Sodium sulfate	21.0	0.7

Table S2. Energy-dispersive X-ray spectroscopy analysis of $Ti_3C_2T_x$ powder before and after intercalation.

Material	**Atomic %**					
	Ti	C	O	F	Cation of electrolyte	S
$Ti_3C_2T_x$	30.0	14.8	16.0	18.9	-	-
$Ti_3C_2T_x$ + KOH	30.0	21.2	30.9	11.4	3.2	-
$Ti_3C_2T_x$ + NaOAc	30.0	16.2	18.2	27.4	5.5	-
$Ti_3C_2T_x$ + K_2SO_4	30.0	17.8	8.4	15.4	1.4	0.0
$Ti_3C_2T_x$ + Na_2SO_4	30.0	17.5	12.9	15.8	1.0	0.0
$Ti_3C_2T_x$ + $MgSO_4$	30.0	29.7	17.0	18.5	0.5	0.1
$Ti_3C_2T_x$ + $MgSO_4$ (electrode)	30.0	59.2*	33.5*	40.0*	2.0	0.0

*Values of the carbon, oxygen and fluorine content are approximate, since spectra were collected from the rolled $Ti_3C_2T_x$ electrode, which contained carbon additive (contributes to C and O content) and PTFE binder (contributes to C, O and F content)

Table S3. Electric conductivity of the aqueous electrolytes used in electrochemical experiments.

Electrolyte	Conductivity, mS/cm
1 M NaOH	141
1 M KOH	191
0.5 M LiOH	90
0.5 M K_2SO_4	100
1 M $(NH_4)_2SO_4$	114
1 M $Mg(NO_3)_2$	115
1 M $MgSO_4$	51
1 M $Al_2(SO_4)_3$	30
1 M $Al(NO_3)_3$	110
3 M NaOAc	79

Table S4. Gravimetric and volumetric specific capacitance data and calculated volumetric and gravimetric energy and power densities of the $Ti_3C_2T_x$ paper electrode in 1M KOH.

Scan rate, mV/s	C, F/cm^3	E, Wh/cm^3	P, W/cm^3	C, F/g	E, Wh/g	P, W/g
2	442	0.0185	0.24	130	0.0055	0.07
5	408	0.0170	0.56	120	0.0051	0.17
10	374	0.0160	1.03	110	0.0046	0.30
20	340	0.0145	1.87	100	0.0042	0.55
50	300	0.0125	4.13	88	0.0037	1.21
100	275	0.0115	7.56	81	0.0034	2.23

References

1. B. Conway, *Electrochemical Supercapacitors: Scientific Fundamentals and Technological Applications* (Kluwer Academic/Plenum, New York, 1999).

2. P. Simon, Y. Gogotsi, Materials for electrochemical capacitors. *Nat. Mater.* **7**, 845–854 (2008). doi:10.1038/nmat2297 Medline

3. I. E. Rauda, V. Augustyn, B. Dunn, S. H. Tolbert, Enhancing pseudocapacitive charge storage in polymer templated mesoporous materials. *Acc. Chem. Res.* **46**, 1113–1124 (2013). doi:10.1021/ar300167h Medline

4. K. Naoi, W. Naoi, S. Aoyagi, J. I. Miyamoto, T. Kamino, New generation "nanohybrid supercapacitor". *Acc. Chem. Res.* **46**, 1075–1083 (2013). doi:10.1021/ar200308h Medline

5. V. Augustyn, J. Come, M. A. Lowe, J. W. Kim, P. L. Taberna, S. H. Tolbert, H. D. Abruña, P. Simon, B. Dunn, High-rate electrochemical energy storage through Li+ intercalation pseudocapacitance. *Nat. Mater.* **12**, 518–522 (2013). doi:10.1038/nmat3601 Medline

6. Z. J. Sun, D. Shu, H. Chen, C. He, S. Tang, J. Zhang, Microstructure and supercapacitive properties of buserite-type manganese oxide with a large basal spacing. *J. Power Sources* **216**, 425–433 (2012). doi:10.1016/j.jpowsour.2012.05.087

7. S. Stankovich, D. A. Dikin, G. H. Dommett, K. M. Kohlhaas, E. J. Zimney, E. A. Stach, R. D. Piner, S. T. Nguyen, R. S. Ruoff, Graphene-based composite materials. *Nature* **442**, 282–286 (2006). doi:10.1038/nature04969 Medline

8. D. Li, M. B. Müller, S. Gilje, R. B. Kaner, G. G. Wallace, Processable aqueous dispersions of graphene nanosheets. *Nat. Nanotechnol.* **3**, 101–105 (2008). doi:10.1038/nnano.2007.451 Medline

9. M. W. Barsoum, T. El-Raghy, The MAX phases: Unique new carbide and nitride materials. *Am. Sci.* **89**, 334 (2001). doi:10.1511/2001.4.334

10. M. Naguib, M. Kurtoglu, V. Presser, J. Lu, J. Niu, M. Heon, L. Hultman, Y. Gogotsi, M. W. Barsoum, Two-dimensional nanocrystals produced by exfoliation of Ti_3AlC_2. *Adv. Mater.* **23**, 4248–4253 (2011). doi:10.1002/adma.201102306 Medline

11. M. Naguib, O. Mashtalir, J. Carle, V. Presser, J. Lu, L. Hultman, Y. Gogotsi, M. W. Barsoum, Two-dimensional transition metal carbides. *ACS Nano* **6**, 1322–1331 (2012). doi:10.1021/nn204153h Medline

12. O. Mashtalir, M. Naguib, B. Dyatkin, Y. Gogotsi, M. W. Barsoum, Kinetics of aluminum extraction from Ti_3AlC_2 in hydrofluoric acid. *Mater. Chem. Phys.* **139**, 147–152 (2013). doi:10.1016/j.matchemphys.2013.01.008

13. O. Mashtalir, M. Naguib, V. N. Mochalin, Y. Dall'Agnese, M. Heon, M. W. Barsoum, Y. Gogotsi, Intercalation and delamination of layered carbides and carbonitrides. *Nature Commun.* **4**, 1716 (2013). doi:10.1038/ncomms2664 Medline

14. J. Come, M. Naguib, P. Rozier, M. W. Barsoum, Y. Gogotsi, P.-L. Taberna, M. Morcrette, P. Simon, A non-aqueous asymmetric cell with a Ti_2C-based two-dimensional negative electrode. *J. Electrochem. Soc.* **159**, A1368–A1373 (2012). doi:10.1149/2.003208jes

15. Q. Tang, Z. Zhou, P. W. Shen, Are MXenes promising anode materials for Li ion batteries? Computational studies on electronic properties and Li storage capability of Ti_3C_2 and $Ti_3C_2X_2$ (X = F, OH) monolayer. *J. Am. Chem. Soc.* **134**, 16909–16916 (2012). doi:10.1021/ja308463r Medline

16. Y. Zhu, S. Murali, M. D. Stoller, K. J. Ganesh, W. Cai, P. J. Ferreira, A. Pirkle, R. M. Wallace, K. A. Cychosz, M. Thommes, D. Su, E. A. Stach, R. S. Ruoff, Carbon-based supercapacitors produced by activation of graphene. *Science* **332**, 1537–1541 (2011). doi:10.1126/science.1200770 Medline

17. L. Mai, H. Li, Y. Zhao, L. Xu, X. Xu, Y. Luo, Z. Zhang, W. Ke, C. Niu, Q. Zhang, Fast ionic diffusion-enabled nanoflake electrode by spontaneous electrochemical pre-intercalation for high-performance supercapacitor. *Sci. Rep.* **3**, 1718 (2013). doi:10.1038/srep01718 Medline

18. P. W. Ruch, M. Hahn, D. Cericola, A. Menzel, R. Kötz, A. Wokaun, A dilatometric and small-angle X-ray scattering study of the electrochemical activation of mesophase pitch-derived carbon in non-aqueous electrolyte solution. *Carbon* **48**, 1880–1888 (2010). doi:10.1016/j.carbon.2010.01.032

19. O. Ghodbane, F. Ataherian, N.-L. Wu, F. Favier, In situ crystallographic investigations of charge storage mechanisms in MnO_2-based electrochemical capacitors. *J. Power Sources* **206**, 454–462 (2012). doi:10.1016/j.jpowsour.2012.01.103

20. S. Murali *et al*., Volumetric capacitance of compressed activated microwave-expanded graphite oxide (a-MEGO) electrodes. *Nano Energy* 10.1016/j.nanoen.2013.01.007 (2013).

21. J. Chmiola, C. Largeot, P.-L. Taberna, P. Simon, Y. Gogotsi, Monolithic carbide-derived carbon films for micro-supercapacitors. *Science* **328**, 480–483 (2010). doi:10.1126/science.1184126 Medline

22. M. Heon, S. Lofland, J. Applegate, R. Nolte, E. Cortes, J. D. Hettinger, P.-L. Taberna, P. Simon, P. Huang, M. Brunet, Y. Gogotsi, Continuous carbide-derived carbon films with high volumetric capacitance. *Energy Environ. Sci.* **4**, 135 (2011). doi:10.1039/c0ee00404a

23. X. Lang, A. Hirata, T. Fujita, M. Chen, Nanoporous metal/oxide hybrid electrodes for electrochemical supercapacitors. *Nat. Nanotechnol.* **6**, 232–236 (2011). doi:10.1038/nnano.2011.13 Medline

24. X. Zhao, L. Zhang, S. Murali, M. D. Stoller, Q. Zhang, Y. Zhu, R. S. Ruoff, Incorporation of manganese dioxide within ultraporous activated graphene for high-performance electrochemical capacitors. *ACS Nano* **6**, 5404–5412 (2012). doi:10.1021/nn3012916 Medline

25. M. Kurtoglu, M. Naguib, Y. Gogotsi, M. W. Barsoum, First principles study of two-dimensional early transition metal carbides. *MRS Commun.* **2**, 133–137 (2012). doi:10.1557/mrc.2012.25

26. M. Khazaei, M. Arai, T. Sasaki, C.-Y. Chung, N. S. Venkataramanan, M. Estili, Y. Sakka, Y. Kawazoe, Novel electronic and magnetic properties of two dimensional transition metal carbides and nitrides. *Adv. Funct. Mater.* **23**, 2185–2192 (2012). doi:10.1002/adfm.201202502

27. J. R. Miller, Valuing reversible energy storage. *Science* **335**, 1312–1313 (2012). doi:10.1126/science.1219134 Medline

28. J. K. McDonough, A. I. Frolov, V. Presser, J. Niu, C. H. Miller, T. Ubieto, M. V. Fedorov, Y. Gogotsi, Influence of the structure of carbon onions on their electrochemical performance in supercapacitor electrodes. *Carbon* **50**, 3298–3309 (2012). doi:10.1016/j.carbon.2011.12.022

29. M. F. El-Kady, V. Strong, S. Dubin, R. B. Kaner, Laser scribing of high-performance and flexible graphene-based electrochemical capacitors. *Science* **335**, 1326–1330 (2012). doi:10.1126/science.1216744 Medline